IEEE Access
Multidisciplinary ⋮ Rapid Review ⋮ Open Access Journal

Received May 23, 2019, accepted June 1, 2019, date of publication June 5, 2019, date of current version June 19, 2019.

Digital Object Identifier 10.1109/ACCESS.2019.2921017

Resilience-Oriented Distribution System Restoration Considering Mobile Emergency Resource Dispatch in Transportation System

YIN XU, (Senior Member, IEEE), YING WANG, (Student Member, IEEE), JINGHAN HE, (Senior Member, IEEE), MINGYU SU, AND PINGHAO NI
School of Electrical Engineering, Beijing Jiaotong University, Beijing 100044, China

Corresponding author: Ying Wang (yingwang1992@bjtu.edu.cn)

This work was supported by the Fundamental Funds for the Central University under Grant 2018RC018.

ABSTRACT After major outages, local power sources, including mobile power sources (MPSs), can be coordinated to serve critical loads in distribution systems (DSs). Repair crews (RCs) are sent to repair faulted components. Both mobile emergency resources, i.e., MPSs and RCs, need to travel through the transportation system (TS) before they reach the destination for service. However, traffic congestion may happen after natural disasters and impact the dispatch of the MPSs and RCs. Therefore, the dynamic traffic state in the TS should be considered for efficient dispatch of mobile emergency resources. This paper proposes a framework to determine critical load restoration strategy for the DS, considering the dispatch strategy of the MPSs and RCs in the TS. The cell transmission model (CTM) is used to formulate the weighted dynamic traffic assignment problem (WDTA) in the TS as a linear program (LP), aiming at minimizing the total prioritized travel time of the MPSs and RCs. For the DS, the multi-period critical load restoration problem (CLR-DS) is formulated as a mixed-integer linear program (MILP) to maximize the cumulated service time to critical loads. Unbalanced three-phase power flow and time-varying topological constraints are considered. Case studies validate the effectiveness of the proposed method.

INDEX TERMS Distribution system, mobile emergency resource, mobile power source, repair crew, resilience, resiliency, service restoration, transportation system.

NOMENCLATURE

A. ABBREVIATIONS

CLR-DS	Critical load restoration model for the distribution system
CTM	Cell transmission model
DG	Distributed generation
DTA	Dynamic traffic assignment
DS	Distribution system
EB	Electric bus
LP	Linear program
MEG	Mobile emergency generator
MESS	Mobile energy storage system
MILP	Mixed-integer linear program
MPS	Mobile power source
RC	Repair crew
TS	Transportation system
WDTA	Weighted dynamic traffic assignment

The associate editor coordinating the review of this manuscript and approving it for publication was Baoping Cai.

B. NOTATION ASSOCIATED WITH THE TRANSPORTATION SYSTEM

SETS AND PARAMETERS

$\mathcal{C}$	Set of all cells, and $\mathcal{C}_O$, $\mathcal{C}_R$, and $\mathcal{C}_S$ are sets of ordinary cells, source cells, and sink cells, respectively
$\mathcal{P}, \mathcal{H}, \mathcal{T}$	Sets of different types of vehicles, cell connectors, and time intervals/periods, respectively
$\mathcal{P}_G, \mathcal{P}_E, \mathcal{P}_B, \mathcal{P}_C$	Sets of MEGs, MESSs, EBs, and RCs, respectively
$\Omega(a)$, $\Omega^{-1}(a)$	Sets of successor cells and predecessor cells to cell a, respectively, $a \in C$
V, V'	Free-flow speed, the speed with which disturbances propagate backward when traffic is congested (the backward wave speed)
$q_{\max}$	Maximum traffic flow
$k_{\max}$	The maximum (or jam) density

V_a Free-flow speed for cell a

$X^0_{a,c}$ Initial flow in cell a for vehicles of type c at the initial time $t = 0$

$Y^0_{(a,b),c}$ Initial flow in the connector (a, b) for vehicles of type c at the initial time $t = 0$

ΔT Duration of each time period

$N^t_{a,\max}$ The maximum amount of flow that can be stored in cell a at time t ($N^t_{a\in\mathcal{C}_R,\max}$ and $N^t_{a\in\mathcal{C}_S,\max}$ are assumed as infinite or a large value)

$Q^t_{a,\max}$ The maximum amount of flow that can flow into or out of cell a during time t ($Q^t_{a\in\mathcal{C}_R}$ and $Q^t_{a\in\mathcal{C}_S}$ are assumed as infinite or a large value)

w_c The weighting factor for vehicle type c

VARIABLES

q Traffic flow

k Traffic density

$x^t_{a,c}$ The flow of vehicles of type c in cell a at time t

$y^t_{(a,b),c}$ The flow of vehicles of type c moving from the cell a to the downstream cell b at time t

V'_a Backward shockwave propagation speed for cell a

δ^t_a Ratio V'_a/V_a for cell a at time t

C. NOTATION FOR THE ELECTRICAL DISTRIBUTION NETWORK

SETS AND PARAMETERS

$\mathcal{N}(t)\mathcal{L}$ Sets of available buses that can be energized at time t, all load buses

$\mathcal{E}(t)$ Set of available lines at time t

$\mathcal{F}$ Set of all faulted zones, $l \in F$

$\mathcal{G}_l$ Set of graphs including buses and lines of a faulted zone that cannot be energized because of faults, $G_l = \langle \mathcal{N}_l, \mathcal{E}_l \rangle$

$\mathcal{N}_{SG}$ Set of all available local DG buses in the post-event distribution system

$\mathcal{N}_G, \mathcal{N}_E, \mathcal{N}_B$ Sets of connection buses for MEGs, MESSs, and EBs, respectively

$\mathcal{S}_G, \mathcal{S}_E, \mathcal{S}_B$ Sets of MEGs, MESSs, and EBs, respectively

α_i/α_{ij} Set of phases of bus i/ line (i, j)

Ω_i Set of adjacent buses of bus i

$i \to j$ The directed line from i to j

$\mathbf{Z}_{ij}$ Impedance matrix of the line (i, j)

w_i The weighting factor of loads at bus i, $w_i \geq 0$

$S_{i,\min}/S_{i,\text{rate}}$ The minimal/rated output power of the DG at bus i

$\boldsymbol{v}_{i,\min}/\boldsymbol{v}_{i,\max}$ Vectors comprised of the square of minimal/ maximal voltage magnitude at bus i in three phases

$\mathbf{s}_{\text{load},i}$ Three-phase load demand of bus i

E^0_i The energy remained in generator i when the outage occurs, $i \in \mathcal{N}_{SG} \cup \mathcal{N}_G$

$p^{\text{ch}}_i, p^{\text{dch}}_i$ The maximum charging power and discharging power of bus i, $i \in \mathcal{N}_E \cup \mathcal{N}_B$

SoC^0_j The initiate SoC of the MESS or EB $j \in \mathcal{S}_E \cup \mathcal{S}_B$

λ_i The parameter of MESS or EB connected to bus i that transforms the energy to SoC

r The root node of the graph

M A large positive real number.

T_l Time for repairing the faulted components in the faulted zone l

$\rho^t_{i,j}$ Whether MPSs is connected to node i at time t: if MPSs j is connected to i at time t, $\rho^t_{i,j} = 1$; otherwise, $\rho^t_{i,j} = 0$

σ^t_i Whether the RCs have arrived at faulted components i at time t: if RCs are arrived at i at time t, $\sigma^t_i = 1$; otherwise, $\sigma^t_i = 0$

VARIABLES

$s^t_{s,i}$ The output of the source of bus i at time t, $s^t_{s,i} = p^t_{s,i} + \mathbf{i}q^t_{s,i}$

$\mathbf{s}^t_i$ A three-dimensional vector variable indicating three-phase power injection of bus i at time t

$\boldsymbol{v}^t_i, \boldsymbol{V}^t_i, \mathbf{i}^t_{ij}$ $\boldsymbol{v}^t_i$ is a complex three-dimensional vector variable indicating the three-phase voltage of bus i at time t, $\boldsymbol{V}^t_i := \boldsymbol{v}^t_i \boldsymbol{v}^{t^H}_i$, $\boldsymbol{i}^t_{ij}$ is a complex three-dimensional vector variable indicating three-phase current of line (i, j) at time t

$\boldsymbol{S}^t_{ij}$ $\boldsymbol{S}^t_{ij} := \boldsymbol{v}^t_i \boldsymbol{i}^{t^H}_{ij}$

$\boldsymbol{\Lambda}^t_{ij}$ A vector variable comprised of diagonal elements of $\boldsymbol{S}^t_{ij}$

γ^t_i Load status at time t: if load i is restored, $\gamma^t_i = 1$; otherwise, $\gamma^t_i = 0$

δ^t_i Source status at time t: if there is a source connected to i and it is on, $\delta^t_i = 1$; otherwise, $\delta^t_i = 0$

a_{ij} Line status: if the line (i, j) is selected to be energized in post-restoration state, $a_{ij} = 1$; otherwise, $a_{ij} = 0$

b_{ij} If node i is the parent of node j in post-restoration state, $b_{ij} = 1$; otherwise, $b_{ij} = 0$

I. INTRODUCTION

Extreme events, including natural disasters, deliberate attacks, and accidents, happened more frequently all over the world in recent years, arising the urgent need for resilience enhancement [1], [2]. The focus of resilience including the metrics [3] and the enhancement measures [4], [5]. Utilizing local power sources for service restoration to critical load in distribution systems is an effective approach to enhance the resilience of the power grid [5], [6]. Distributed generations (DGs) [7], microgrids [8]–[13], and networked microgrids [14], [15] are used for critical load restoration.

Specifically, mobile power sources (MPSs) are flexible to be connected at any suitable buses, usually close to critical loads, to facilitate the restoration process. In addition, repair crews (RCs) can be sent to repair faulted components in the distribution systems to provide more restoration paths. In this paper, MPSs and RCs are referred to as mobile emergency resources.

The mobile emergency resources should be dispatched to the desired locations through the transportation system (TS). The state of traffic flow in the TS, such as congestion, has a significant impact on the dispatch of mobile emergency resources and further affects the restoration process in the DS. Therefore, the dispatch strategy of mobile emergency resources in the TS, including scheduling and routing [16], is essential and should be considered when deciding the restoration strategy in the DS.

Research has been done to optimally dispatch the mobile emergency resources in the TS [17]–[24]. In [17], the routing and scheduling of MPSs are obtained by a two-stage framework. In [19], a pre-positioning and real-time allocation method of mobile emergency generators (MEGs) is proposed, and the MEGs are dispatched through the shortest paths between the origins and destinations. The shortest paths are selected to obtain travel time of mobile energy storage systems (MESSs) for resilience enhancement in [20]. In [21], a two-stage method is proposed to deal with the outage management with RCs, reconfiguration, and DG dispatch. The dispatch of RCs and MPSs in the above work is modeled based on graph theory and the travel time is determined by travel distance. In [22], the routing of MPSs is determined by the Dijkstra algorithm and the travel time is modeled as a random variable by a stochastic framework based on unscented transform. In [23], the transportation network with travel time is modeled by a time-space network regardless of the traffic flow state in the TS. To the best of our knowledge, the study on mobile emergency resource dispatch for service restoration in the DS considering the real-time traffic flow state in the TS has not been reported.

In some recent studies, the dispatch of mobile emergency resources is considered in determining the distribution system restoration strategy. In [21], the distribution system restoration problem is formulated as a mixed-integer linear program to maximize the picked-up loads and minimize the repair time, in which the routing of repair crews is considered. In [22], the truck-mounted mobile emergency sources are sent to deliver power to the islanded outage area, and networked microgrids are formed. In [23], a joint post-disaster restoration scheme considering the schedule of MESSs is proposed to minimize the total system cost including customer interruption cost, generation cost, and MESSs related costs. In the scheme, MESSs are dynamically scheduled in coordination with DS reconfiguration through microgrids.

In this paper, resilience-oriented service restoration framework for the DS considering dispatch of mobile emergency resources in the TS is proposed. The major contributions include:

1) A framework to determine the multi-period critical load restoration strategy considering mobile emergency resources dispatch in the TS is proposed, and the dynamic traffic flow in the TS is considered to determine the dispatch of MPSs and RCs.
2) The weighted dynamic traffic assignment model (WDTA) considering the priority of different types of vehicles such as MPSs and RCs, is formulated as a linear program (LP) to minimize the weighted travel time of different types of vehicles in the TS.
3) The multi-period critical load restoration problem for the DS (CLR-DS) is formulated as a mixed-integer linear program (MILP), considering the dispatch of mobile emergency sources and time-varying topology of distribution network due to repair.

The remainder of this paper is organized as follows. Section II describes the problem of service restoration considering the dispatch of mobile emergency resources. The framework to determine the critical load restoration strategy is proposed in Section III. Sections IV and V present the WDTA model for the TS and critical load restoration model for the DS, respectively. Numerical results are presented in Section VI. Section VII concludes the paper.

II. PROBLEM DESCRIPTION

It is assumed that after a major outage, the utility power is not available for the DS. The local power sources, including local DGs and MPSs, are used for service restoration in the DS. MPSs include the utility-owned MESSs, MEGs [17], and electric buses (EBs) [18]. Note that power sources may be damaged during an extreme event. Damage of power sources will result in a lack of generation capacity and reduce the amount of load that can be restored. An availability-based resilience evaluation method is proposed in [3] to quantify this effect. Preventing power sources from damage is essential for load restoration in the DS. In addition, RCs are sent to repair damaged components in the DS to accelerate the restoration process. The mobile emergency resources have to travel through the TS from origin points to their destinations. It is assumed that the origin points and destinations are known, which can be determined by the pre-positioning and real-time allocation methods proposed by papers such as [18] and [19]. The multi-period restoration strategy in the DS should consider the travel time of MPSs and RCs, and the repair time of damaged components.

An example of a DS with the corresponding TS is shown in Fig. 1 [24]. In Fig. 1, the two systems are geographically corresponding to each other. The TS is in a metropolitan area with ring expressways, such as Beijing. After a disaster, two expressways between node 6 and 10 is broken, and multiple faults occur in the DS and the utility power is unavailable.

For the TS, the word "O" denotes the origin nodes and "D" the destination nodes. The "shelter", with enough space, is the destination of the ordinary vehicles. The ordinary vehicles are personal vehicles on the road when the disaster happens. The spare EBs in the bus depots can be dispatched

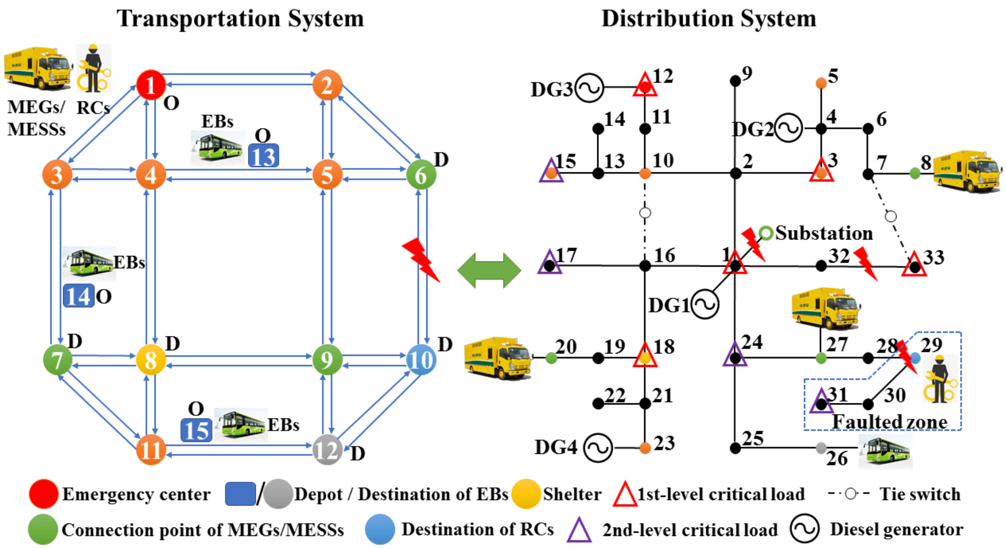

FIGURE 1. An illustration of the DS and the corresponding TS after a disaster.

to the plots which have the Vehicle to Grid ability, referred to as the ''destination of EB''. The MEGs, MESSs, and RCs are sent from the ''emergency center.'' There are only several ''connection points'' of MPS which are equipped with supporting facilities such as MESS stations, etc. The ''destination of RC'' indicates the locations of damaged components in the DS which needs to be repaired quickly.

In the DS, the electric critical loads, such as hospitals, water stations, etc., can be divided into several levels considering their importance. The tie lines provide flexible reconfiguration for restoration. The network is divided into several parts by the multiple faults. As to the critical load restoration in the DS, the idea of multiple sources coordination [11] is utilized to interconnect available power sources for restoring more critical load. The largest island that can be formed by closing switches to interconnect all available power sources is referred to as the ''main zone'', and the ''faulted zone'' is referred to the islanded zone that cannot be energized because of faults, as shown in Fig. 1. The faulted zone can be energized after the corresponding faulted component repaired during the restoration process.

For the DS, considering the dispatch of mobile emergency resources in the TS, the optimal multi-period critical load restoration strategy during the outage is needed, to determine the set of loads to be served and the service time, the radial topology, and the outputs of all power sources; for the TS, the traffic assignment strategy is needed to determine the dynamic traffic flow to ensure the timely arrival of mobile emergency resources.

Assume that the emergency center has the responsibility to make comprehensive decisions on the traffic assignment strategy in the TS and the service restoration strategy in the DS. In addition, it is able to send order signals to each vehicle to remotely control the traffic flow for system optimum, and can also remotely control all electric components in the DS [25]. The task of the emergency center is shown in Fig. 2.

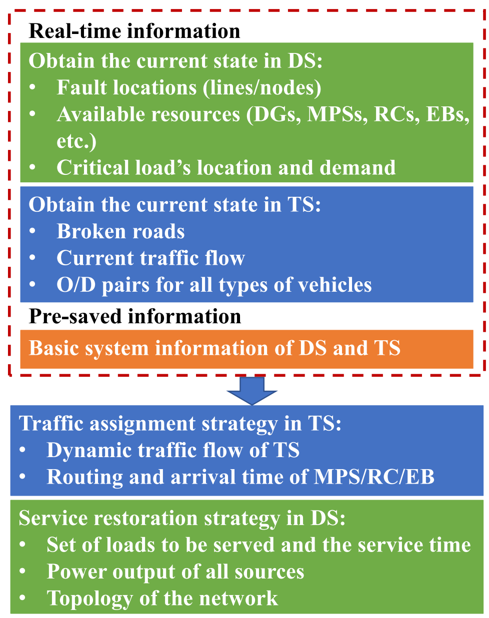

FIGURE 2. The task of the emergency center for emergency response.

The challenges of the service restoration problem considering dispatch of mobile emergency resources in the TS lie in two aspects: 1) how to model the impact of real-time traffic state on the dispatch of mobile emergency resources; 2) the decisions should be obtained online to realize real-time emergency response. The rest of this paper will focus on the methods to tackle these issues.

III. RESTORATION FRAMEWORK

In this section, a two-step restoration framework is proposed to make decisions on multi-period restoration strategy for the DS considering dispatch of mobile emergency resources in the TS.

Based on the logic of the decisions of two systems, the whole decision-making process is divided into two steps:

Step 1: Determine routes and travel time of mobile emergency resources by solving the weighted dynamic traffic assignment problem the TS;

Step 2: Based on the results of Step 1, decide the multi-period critical load restoration strategy in the DS.

The inputs and outputs of the two steps and their relationship are shown in Fig. 3.

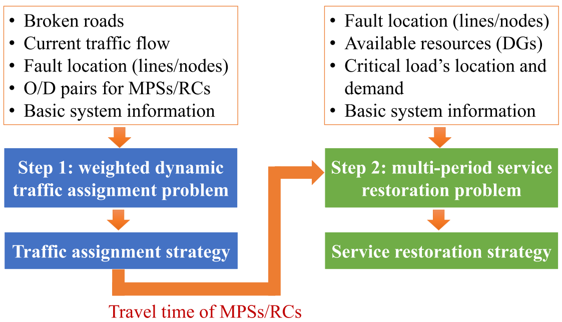

FIGURE 3. The procedure of the proposed restoration framework.

For the MPSs, the travel time of them decides when they can be used for service restoration. For the faulted components, the travel time of RCs and the time for repair decide when the corresponding components will be available for load restoration. The travel time of MPSs and RCs provided in Step 1 are the inputs of the DS service restoration model in Step 2, as shown in Fig. 3.

In Step 1, the dynamic traffic assignment in the TS should be determined, minimizing the total weighted travel time of different types of vehicles. The dispatch strategy, including routing and arrival time of all mobile emergency resources, are determined. The mathematical formulation of this problem is presented in Section IV.

In Step 2, for critical load restoration problem in the DS, the objective is to maximize the cumulated service time for loads, weighted by their priority, subject to unbalanced power flow equations, security operational constraints, and topological constraints. In this paper, the multi-period critical load restoration problem for the DS is formulated as a MILP, presented in Section V.

IV. TRANSPORTATION SYSTEM MODELING

DTA model is used to simulate the spatial and temporal distributions of traffic flows [26]. In this paper, the WDTA considering the priority of vehicles is proposed to minimize the total weighted travel time of different types of vehicles. The proposed WDTA is based on cell transmission model (CTM). In this section, the CTM is briefly introduced and then the specific formulation of WDTA.

A. CELL TRANSMISSION MODEL

CTM is the discrete-time approximation of differential Lighthill-Whitham-Richards equations by assuming a piecewise linear relationship between flow and density at the cell level [27], [28]. It can represent the traffic propagation on a TS and describe the traffic dynamic phenomena [29].

The initiator of this model showed that, if the relationship between traffic flow (q) and density (k) satisfies the equation

$$q = \min\left\{Vk, q_{\max}, V^{'}\left(k_{\max} - k\right)\right\}, \tag{1}$$

the time could be discretized into small intervals, and based on that, every link of the TS can be divided into cells, i.e., CTM in the TS. In a specific time duration of interest, a time interval is defined to divide the duration to several intervals. The length of each cell is equal to the distance traveled by free-flow moving vehicles in the time interval. In this paper, cells are divided into three kinds: source cells, ordinary cells, and sink cells. The classification of cells is shown in Fig.4 [28].

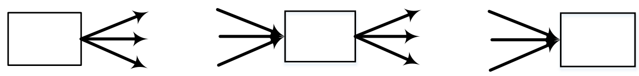

(a) (b) (c)

FIGURE 4. Classification of cells. (a) Source cell. (b) Ordinary cell. (c) Sink cell.

The evolution of traffic flow can be expressed as follows:

$$x_a^t = x_a^{t-1} + \sum\nolimits_{b\in\Omega^{-1}(a)} y_{(b,a)}^{t-1} - \sum\nolimits_{b\in\Omega(a)} y_{(a,b)}^{t-1}, \quad \forall a \in \mathcal{C}, \forall t \in \mathcal{T}\{0\} \tag{2}$$

$$\sum\nolimits_{b\in\Omega(a)} y_{(a,b)}^t \leq \min\left\{x_a^t, Q_{a,\max}^t\right\}, \forall a \in \mathcal{C}, \forall t \in \mathcal{T} \tag{3}$$

$$\sum\nolimits_{b\in\Omega^{-1}(a)} y_{(b,a)}^t \leq \min\left\{Q_{a,\max}^t, \delta_a^t\left(N_{a,\max}^t - x_a^t\right)\right\}, \forall a \in \mathcal{C}, \forall t \in \mathcal{T} \tag{4}$$

Equation (2) is the flow conservation at each cell, where for source cell a, $\Omega^{-1}(a) = \emptyset$ and for sink cell a, $\Omega(a) = \emptyset$. Inequations (3)–(4) are derived from (1) and applicable for all kinds of cells.

B. WEIGHTED DYNAMIC TRAFFIC ASSIGNMENT

In the TS, there are four types of vehicles after disasters: MPSs, RCs and ordinary vehicles. The origin and destination points for different types of vehicles are described in Section II. The objective of the WDTA in this paper is minimizing the total weighted travel time of all types of vehicles considering their priority. The constraints include the traffic flow conservation constraint and the constraints derived by (1). The specific model is as follow.

WDTA:

$$\min f_1 = \sum_{c\in\mathcal{P}} \sum_{t\in \mathrm{T}} \sum_{a\in\mathcal{C}\setminus\mathcal{C}_R} w_c\left(\sum\nolimits_{c\in\mathcal{P}} x_{a,c}^t\right)$$

$$\text{over } x_{a,c}^t \in \mathbb{R}^+, \text{for } a \in \mathcal{C}, c \in P, t \in \mathcal{T}$$
$$y_{(a,b),c}^t \in \mathbb{R}^+, for(a,b) \in \mathcal{H}, c \in \mathcal{P}, t \in \mathcal{T} \quad (5)$$
$$s.t.\ x_{a,c}^t = x_{a,c}^{t-1} + \sum\nolimits_{b\in\Omega^{-1}(a)} y_{(b,a),c}^{t-1} - \sum\nolimits_{b\in\Omega(a)} y_{(a,b),c}^{t-1}, \quad a \in \mathcal{C}, t \in T\,\{0\}, c \in \mathcal{P} \quad (5a)$$
$$\sum\nolimits_{b\in\Omega(a)} y_{(a,b),c}^t \le x_{a,c}^t, a \in \mathcal{C}, t \in T, c \in \mathcal{P} \quad (5b)$$
$$\sum\nolimits_{c\in\mathcal{P}} \sum\nolimits_{b\in\Omega(a)} y_{(a,b),c}^t \le Q_{a,\max}^t, a \in \mathcal{C}, t \in \mathcal{T} \quad (5c)$$
$$\sum\nolimits_{c\in \mathrm{P}} \sum\nolimits_{b\in\Omega^{-1}(a)} y_{(b,a),c}^t \le Q_{a,\max}^t, a \in \mathcal{C}, t \in \mathcal{T} \quad (5d)$$
$$\sum\nolimits_{c\in \mathrm{P}} \sum\nolimits_{b\in\Omega^{-1}(a)} y_{(b,a),c}^t \le \delta_a^t \left(N_{a,\max}^t - \sum\nolimits_{c\in\mathcal{P}} x_{a,c}^t\right), \quad a \in \mathcal{C}, t \in \mathcal{T} \quad (5e)$$
$$x_{a,c}^0 = X_{a,c}^0, y_{(a,b),c}^0 = Y_{(a,b),c}^0, \quad a \in \mathcal{C}, (a,b) \in \mathcal{H}, c \in \mathcal{P} \quad (5f)$$

The objective is to minimize the total weighted travel time of all types of vehicles. In each cell, the travel time of vehicles has a nonnegative correlation with the density, namely x_a, so f_1 is to minimize the total weighted travel time of all types of vehicles in the whole duration. Constraints (5a) is the traffic flow conservation constraints. Constraints (5b)–(5e) are the transformation of (1). Constraint (5b) represents that the total flow of vehicles of type c moving from cell a to other cells is not larger than the flow of vehicles of type c in cell a. Constraint (5c) indicates that the total flow moving from cell a to other cells is not larger than the maximum capacity of cell a. Constraint (5d) shows that the total flow moving to cell a from other cells is not larger than the maximum capacity of cell a. Constraint (5e) states that the total inflows of cell a do not exceed the available residual occupancy of that cell. This constraint deals with the situation when the traffic is congested [24]. To sum up, (5b), (5c)–(5d), and (5e) are corresponding to the three terms on the right side of (1). Constraint (5f) is the initial state of flow in cells and connectors. In this paper, in the initial state, the ordinary vehicles are in cells excluding sink and source cells, indicating they are on the roads when the event occurs. Others are in source cells. In addition, there is no flow in connectors at the beginning.

C. SOLUTION METHOD

It can be seen that the model WDTA is an LP, which can be solved by the interior-point algorithm or the simplex algorithm, with global optimum guaranteed. The optimization algorithms are integrated into many off-the-shelf optimization solvers such as MOSEK or CPLEX. In this paper, the LP problem is modeled in MATLAB R2016a with the CVX package [31] and solved by the optimization solver MOSEK [32].

After solving the WDTA, the routing and arrival time of all mobile emergency resources can be determined.

V. MULTI-PERIOD CLR MODEL FOR THE DS

For the DS, a multi-period critical load restoration model for the DS (CLR-DS) considering dispatch of mobile emergency resources is proposed. The entire outage duration is evenly divided into several periods, indexed by t. The specific objective and constraints are introduced as follows.

A. OBJECTIVE

The objective is maximizing the cumulated service time for loads, weighted by their priority, as shown in (4).

$$\max f_2 = \sum\nolimits_{t\in\mathcal{T}} \sum\nolimits_{i\in\mathcal{L}} w_i \gamma_i^t \quad (6)$$

In fact, the cumulative service time is $\sum_{t\in\mathcal{T}} \sum\limits_{i\in\mathcal{L}} w_i\gamma_i^t \Delta T$. ΔT is omitted because it is a constant.

B. CONSTRAINTS

1) OPERATIONAL CONSTRAINTS

The operational constraints include unbalanced three-phase power flow equation, voltage limits, and power output and energy limits of local DGs, as shown below.

$$\sum\nolimits_{k:k\to i} \boldsymbol{\Lambda}_{ki}^t + \boldsymbol{s}_i^t = \sum\nolimits_{j:i\to j} \boldsymbol{\Lambda}_{ij}^t, i \in \mathcal{N}(t), t \in \mathcal{T} \quad (6a)$$
$$\boldsymbol{S}_{ij}^t = \boldsymbol{r}\mathrm{DIAG}\left(\boldsymbol{\Lambda}_{ij}^t\right), i \to j \in \mathcal{E}(t), t \in \mathcal{T} \quad (6b)$$
$$\begin{cases} -(1-a_{ij})\mathrm{M} \le \boldsymbol{V}_i - \boldsymbol{V}_j^t - \left(\boldsymbol{Z}_{ij}^H \boldsymbol{S}_{ij}^t + \boldsymbol{S}_{ij}^{t^H} \boldsymbol{Z}_{ij}\right) \\ \boldsymbol{V}_i - \boldsymbol{V}_j^t - \left(\boldsymbol{Z}_{ij}^H \boldsymbol{S}_{ij}^t + \boldsymbol{S}_{ij}^{t^H} \boldsymbol{Z}_{ij}\right) \le (1-a_{ij})\mathrm{M}, \end{cases} \quad i \to j \in \mathcal{E}(t), t \in \mathcal{T} \quad (6c)$$
$$\begin{cases} -a_{ij}\left(\mathrm{M} + \boldsymbol{j}\mathrm{M}\right) \cdot ones(3,1) \le \boldsymbol{\Lambda}_{ij}^t \\ \boldsymbol{\Lambda}_{ij}^t \le a_{ij}\left(\mathrm{M} + \boldsymbol{j}\mathrm{M}\right) \cdot ones(3,1), \end{cases} \quad i \to j \in \mathcal{E}(t), t \in \mathcal{T} \quad (6d)$$
$$\mathrm{sum}\left(\boldsymbol{s}_i^t + \boldsymbol{s}_{\mathrm{load},i}\gamma_i^t\right) = s_{\mathrm{s},i}^t, i \in \mathcal{N}(t), t \in \mathcal{T} \quad (6e)$$
$$\boldsymbol{v}_{i,\min} \le \mathrm{diag}(\boldsymbol{V}_i^t) \le \boldsymbol{v}_{i,\max}, i \in \mathcal{N}(t), t \in \mathcal{T} \quad (6f)$$
$$\delta_i^t S_{i,\min} \le s_{\mathrm{s},i}^t \le \delta_i^t S_{i,\mathrm{rate}}, i \in \mathcal{N}_{SG}, t \in \mathcal{T} \quad (6g)$$
$$\mathrm{real}(\sum\nolimits_{t\in T} \Delta \mathrm{T} s_{\mathrm{s},i}^t) \le \mathcal{E}_i^0, i \in \mathcal{N}_{SG} \quad (6h)$$

where the function DIAG(·) returns a diagonal matrix with diagonal elements are the input vector, the function diag(·) returns a vector comprised of diagonal elements of the input matrix, and function ones(m, n) returns an m × n matrix of ones; $r = \begin{bmatrix} 1 & \alpha^2 & \alpha \\ \alpha & 1 & \alpha^2 \\ \alpha^2 & \alpha & 1 \end{bmatrix}$ where $\alpha = e^{-\frac{2\pi}{3}j}$.

Constraints (6a)–(6c) are linear approximation model [33] for unbalanced power flow constraints. Equation (6a) represents that the sum of power flowing into bus i equals that out of bus i, (6b) the relationship between $\mathbf{S}_{ij}^t$ and $\boldsymbol{\Lambda}_{ij}^t$, and (6c) the voltage difference of two node on line $i\to j$. Note that the "Big

M'' method is used to represent two conditions when the line $i \rightarrow j$ is energized or not. Equation (6d) means that if the line $i \rightarrow j$ is not energized ($a_{ij} = 0$), the power flow of $i \rightarrow j$ is 0. Constraint (6e) shows that the injection power of bus i plus the load demand of i is equal to the power generation of the DG connected to i. Constraint (6f) is the voltage limits and (6g) represents the power output limits. In this paper, the local DGs considered are all controllable generators. Constraint (6h) is the energy limits indicating that the fuel, such as diesel or gas, remained in a DG is limited.

2) MOBILE SOURCE CONSTRAINTS

The mobile source constraints include the relevant constraints on MEGs, MESSs, and EBs. The specific constraints are as follows.

$$\delta_i^t \sum\nolimits_{j \in S_G} \rho_{i,j}^t S_{i,\min} \leq s_{s,i}^t \leq \delta_i^t \sum\nolimits_{j \in \mathcal{S}_G} \rho_{i,j}^t S_{i,\text{rate}}, \quad i \in \mathcal{N}_G, t \in \mathcal{T} \tag{6i}$$

$$\text{real}(\sum\nolimits_{t \in \mathcal{T}} \Delta T s_{s,i}^t) \leq \sum\nolimits_{j \in \mathcal{N}_G} \rho_{i,j}^{|\mathcal{T}|} E_j^0, i \in \mathcal{N}_G \tag{6j}$$

$$-\delta_i^t \sum\nolimits_{j \in \mathcal{S}_E} \rho_{i,j}^t p_j^{\text{ch}} \leq p_{s,i}^t \leq \delta_i^t \sum\nolimits_{j \in \mathcal{S}_E} \rho_{i,j}^t p_j^{\text{dch}}, \quad i \in \mathcal{N}_E, t \in \mathcal{T} \tag{6k}$$

$$\sum\nolimits_{j \in \mathcal{S}_E} \rho_{i,j}^t SoC_{j,\min} \leq \sum\nolimits_{j \in \mathcal{S}_E} \rho_{i,j}^t SoC_{j,0} - \sum\nolimits_{t=1}^{t'} \Delta T \lambda_i p_{s,i}^t \leq \sum\nolimits_{j \in \mathcal{S}_E} \rho_{i,j}^t SoC_{j,\max}, \quad i \in \mathcal{N}_E, t' \in \mathcal{T} \tag{6l}$$

$$-\delta_i^t \sum\nolimits_{j \in \mathcal{S}_B} \rho_{i,j}^t p_j^{\text{ch}} \leq p_{s,i}^t \leq \delta_i^t \sum\nolimits_{j \in \mathcal{S}_B} \rho_{i,j}^t p_j^{\text{dch}}, \quad i \in \mathcal{N}_B, t \in \mathcal{T} \tag{6m}$$

$$\sum\nolimits_{j \in \mathcal{S}_B} \rho_{i,j}^t SoC_{j,\min} \leq \sum\nolimits_{j \in \mathcal{S}_B} \rho_{i,j}^t SoC_{j,0} - \sum\nolimits_{t=1}^{t'} \Delta T \lambda_i p_{s,i}^t \leq \sum\nolimits_{j \in \mathcal{S}_B} \rho_{i,j}^t SoC_{j,\max}, \quad i \in \mathcal{N}_B, t' \in \mathcal{T} \tag{6n}$$

Constraints (6i)–(6j) are for MEGs and corresponding to (6g)–(6h), i.e., the power output and energy limits. The parameters $\rho_{i,j}^t$ and σ_i^t are determined by the arrival time of the MPSs and RCs, respectively. Constraint (6i) means that the power output at the bus i does not exceed the total maximum power outputs of all MEGs connecting to bus i. (6j) indicates that the energy consumed through bus i does not exceed the total energy stored in all MEGs. $|\mathcal{T}|$ is the total number of time periods. Constraints (6k)–(6l) and (6m)–(6n) are the power and state of charging (SoC) constraints for MESSs and EBs. Constraint (6k) and (6m) indicate that the power at bus i is between total negative maximal charging power and maximal discharging power of all MESSs or EBs connecting to bus i. For safe and economic operating of energy storage devices, the SoC of them should be maintained in a specific range. Therefore, the SoC constraints (6l) and (6n) are considered.

3) TOPOLOGICAL CONSTRAINTS

During the restoration process, the radial topology should be maintained and the topology of the network will be dynamically changed when some faults are repaired during restoration. The specific model is as follows.

$$b_{rj} = 0, \quad \forall (1, j) \in \cup_{t \in \mathcal{T}} \mathcal{E}(t) \tag{6o}$$

$$\sum\nolimits_{j \in \Omega_i} b_{ij} = 1, \quad \forall (i, j) \in \cup_{t \in \mathcal{T}} \mathcal{N}(t)/\text{r} \tag{6p}$$

$$b_{ij} + b_{ji} = a_{ij}, \quad \forall (i, j) \in \cup_{t \in \mathcal{T}} \mathcal{E}(t) \tag{6q}$$

$$\mathcal{N}(t + T_l) = \mathcal{N}(t + T_l - 1) \cup \sigma_i^t \mathcal{N}_l, \quad i \in \mathcal{N}_l, l \in \mathcal{F}, t \in \mathcal{T} \tag{6r}$$

$$\mathcal{E}(t + T_l) = \mathcal{E}(t + T_l - 1) \cup \sigma_i^t \mathcal{E}_l \quad i \in \mathcal{N}_l, l \in \mathcal{F}, t \in \mathcal{T} \tag{6s}$$

Constraints (6o)–(6q) are the spanning tree constraints indicating a radial topology. The radial topological constraint is for the whole post-restoration distribution network. The parameter r in (6o) and (6p) represents the root node in the spanning tree. Constraint (6o) indicates that the root node has no parent node and (6p) says that each node except the root node in a spanning tree has only one parent node. Constraint (6q) shows that if node i and node j have a parent-child relationship, the line (i, j) is connected (a_{ij}) in the post-restoration network.

Constraints (6r)–(6s) represent that the topology expends because some faulted components are repaired during restoration. At the beginning of the restoration, the network $\mathcal{G}(t) = \langle \mathcal{N}(t), \mathcal{E}(t) \rangle$ is the main zone. Once a faulted component corresponding to a faulted zone l is repaired at $t + 1$, the topology will become $\mathcal{G}(t+1) = \langle \mathcal{N}(t) \cup \mathcal{N}_l, \mathcal{E}(t) \cup \varepsilon_l \rangle$, as (6r) and (6s) indicated. In (6r) and (6s), T_l is the time for repairing the faulted component in the faulted zone l. Equation (6r) indicates that after the RCs' arrival, it will take T_l before the set of buses including the faulted zone l. Similar to (6r), (6s) means that the set of lines can include the faulted zone l after RCs repair the faulted component.

4) INTEGER-ASSOCIATED Constraints

Considering the meanings of the time-related integer variables, some constraints should be added to make it reasonable and practical. The constraints are as follows.

$$\gamma_i^t \geq \gamma_i^{t-1}, i \in \mathcal{L}, t \in \mathcal{T}/1 \tag{6t}$$

$$\delta_i^t \leq \delta_i^{t-1}, i \in \mathcal{N}_{SG} \cup \mathcal{N}_G \cup \mathcal{N}_E \cup \mathcal{N}_B, t \in \mathcal{T}/1 \tag{6u}$$

Constraint (6t) represents that the load is not allowed to be shed after restored. Constraint (6u) represents that it is preferred that the sources at node i are used for restoration until the energy is used up.

TABLE 1. Parameters of the TS.

Links	Length (km)	Free speed (km/h)	Max. flow (vph)
1-2, 6-10, 12-11, 7-3	12	72	1440
1-3,2-6, 10-12, 11-7	6	72	1440
4-5, 5-9, 9-8, 8-4	12	72	720
1-4,3-4, 2-5, 5-6, 9-10, 9-12, 8-11, 8-7	6	72	720

TABLE 2. Local DGs data in the DS.

Gen. (#)	BUS (#)	$p_{\min}$ (kW)	$p_{\max}$ (kW)	$q_{\min}$ (kVar)	$q_{\max}$ (kVar)	Energy (kWh)
1	1	150	600	-350	500	200
2	4	30	100	-30	50	100
3	12	50	150	-50	80	100
4	23	30	100	-30	50	100

C. CLR-DS FORMULATION AND SOLUTION METHOD

To sum up, the multi-period critical load restoration problem for the DS is formulated as follow.

$$\begin{aligned}
&\textbf{CLR-DS}: \max f_2\\
&\text{over } \gamma_i^t \in \{0,1\} \text{ for } i \in \mathcal{L}, t \in \mathcal{T};\\
&\quad \delta_i^t \in \{0,1\} \text{ for } i \in \mathcal{N}_{SG} \cup \mathcal{N}_G \cup \mathcal{N}_E \cup \mathcal{N}_B, t \in \mathcal{T};\\
&\quad a_{ij}, b_{ij}, b_{ji} \in \{0,1\} \text{ for } (i,j) \in U_{t\in\mathcal{T}}\mathcal{E}(t);\\
&\quad \mathbf{s}_i^t \in \mathbb{C}^{|\alpha_i|}, V_i^t \in \mathbb{H}^{|\alpha_i|\times|\alpha_i|} \text{ for } i \in \mathcal{N}(t), t \in \mathcal{T};\\
&\quad \mathbf{S}_{ij}^t \in \mathbb{C}^{|\alpha_{ij}|\times|\alpha_{ij}|} \text{ for } (i,j) \in \mathcal{E}(t), t \in \mathcal{T}\\
&s.t.\ (6a) - (6u)
\end{aligned}$$

The model CLR-DS is a MILP. As a mixed-integer program, the MILP can be solved by the branch-and-bound algorithm or the cutting plane approach. The optimization algorithms are integrated into many off-the-shelf optimization solvers such as MOSEK or CPLEX. In this paper, the MILP problem is modeled in MATLAB R2016a with the CVX package [31] and solved by the optimization solver MOSEK [32].

VI. CASE STUDIES

The proposed restoration framework has been implemented in MATLAB R2016a with the CVX package [31]. The linear program and mixed integer linear program are solved using the optimizer in MOSEK [32]. The numerical experiments are carried out on a personal computer with Intel Core I5 CPU at 2.40 GHz with 8 GB of RAM. The DS and the TS showed in Fig. 1 is used to validate the proposed method.

A. TEST SYSTEM INFORMATION

As shown in Fig. 1, the TS has 12 nodes and 20 links. Node 1 is the emergency center representing the origin point of MEGs, MESSs, and RCs. The three rectangles are the depots of EBs, i.e., the origin points of EBs. Node 6 and node 7 are the destinations of MEGs, node 9 the destination of MESSs and node 10 the destination of RCs. The basic parameters of the roads in the TS are given in Table 1.

In Table 1, the last entry "Max. flow" indicates that the maximum service flow rate, whose unit is vehicles per hour (vph). We can see that the outer ring expressways have larger capacities to carry more traffic flows.

For the DS, four local DGs are integrated and parameters of them are provided in Table 2. Two tie lines, 10–16 and 7–33, provide topology flexibility. The electric power loads are clarified into three levels considering the importance. Buses 3, 12, and 33 are 1st-level critical loads with weighting factor 100, and 15, 17, 24, and 30 are 2nd-level critical loads with 10, and others are regular loads with 0.2. Parameters of loads and lines are given in the Appendix.

In Table 2, the entry "Energy" is the remained energy in the generator. In this paper, the local DGs are all diesel generators and the remained energy indicate the amount of diesel fuel stored in the generator.

As to the mobile emergency resources, including MEGs, MESSs, RCs, and spare EBs, the numbers of vehicles of them are 8, 4, 4, and 25, respectively. The 25 EBs are distributed at three bus depots, 13, 14, and 15, the numbers are 7, 8, and 10, respectively. The parameters of each mobile source are listed in Table 3.

TABLE 3. The parameters of each mobile source.

Type	$p_{\min}$ /$p_{\max}$ (kW)	$q_{\min}$ /$q_{\max}$ (kVar)	Energy (kWh)	Energy Capacity (kWh)	$SoC_{\min}$ (p.u.)	$SoC_{\max}$ (p.u.)
MEG	30/100	-30/50	300	/	/	/
MESS	∓100	∓40	200	250	0.9	0.1
EB	∓100	∓40	120	150	0.9	0.1

Assume that an extreme disaster attacked the test system, and the two expressways between 6 and 10 are broken in the TS. The DS is experiencing an outage and disconnected with the substation. Two faults occurred at node 32 and 29, thus a faulted zone is formed comprised by nodes 29, 31, 30 and the lines between them. In addition, the prediction time for transmission system restoration is 4h. In this situation, the emergency center has the responsibility to respond immediately to restore the service of the DS. The emergency resource demands in the DS, including the number and origin-destination (O-D) pairs of each type of mobile resources, are listed in Table 4. The repair time for the faulted component at bus 29 is 25min.

In Table 4, the entry "number" means the number of vehicles of the corresponding type of mobile resources.

B. RESULTS

The proposed restoration framework is applied to make decisions on the multi-period restoration strategy considering dispatch of mobile emergency resources in the TS. The results are presented step by step.

TABLE 4. The number and O-D pairs of each type of mobile resources.

Type	Number	Origin point (#)	Destination (#)
MEG	4	1	6
	4	1	7
MESS	4	1	9
RC	4	1	10
	7	13	12
EB	8	14	12
	10	15	12

1) Step 1: Determine the Traffic Assignment Strategy

In the TS, if all roads are considered, the number of cells will be excessive and the problem will be more complicated. We can see that the most mobile emergency resources have to travel from the northwest to the east and south, so the critical roads are selected to be divided into cells to study the routing and schedule of mobile emergency resources, as illustrated in Fig. 5 [26].

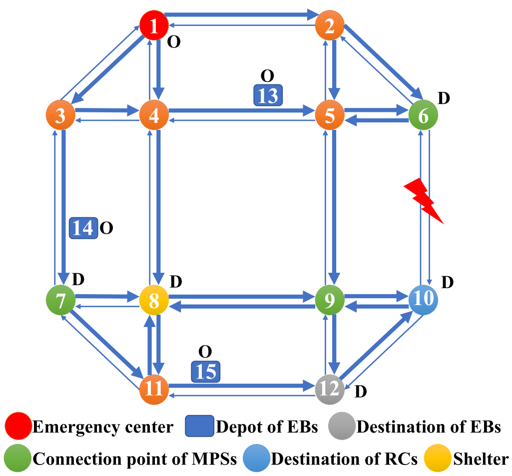

FIGURE 5. The simplified the TS network.

In Fig. 5, the bold links are the selected roads that are considered to study the traffic assignment strategy for mobile emergency resources. The time interval is 5 min thus the length of a cell is 6 km, and the total duration is 1h. The TS is divided into 41 cells, as depicted in Fig. 6.

In Fig. 6, the origin and destination points are marked with different colors, and these are the source and sink cells. The cell properties are illustrated in Table 5.

TABLE 5. Cell properties.

Properties	Cell (#)
$N_{a,\max} = 100000, Q_{a,\max} = 100000$	1,11,23,29,30,33,38-41
$N_{a,\max} = 1200, Q_{a,\max} = 720$	2-4,14,16,17,22,27,28,37
$N_{a,\max} = 600, Q_{a,\max} = 360$	5-10,12,13,15,18-21,23-26,31,32,34-36

According to the parameters listed in Table 1 and the time interval, the properties of cells can be obtained, including

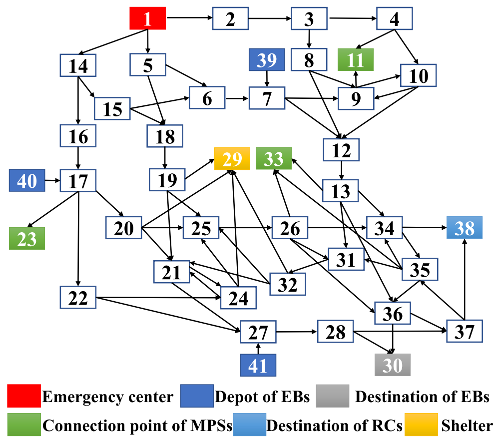

FIGURE 6. CTM representation of the TS.

the maximum amount of flow that can be stored in a cell $N_{a,\max}$ and the maximum amount of flow that can flow into or out of the cell $Q_{a,\max}$. For the sources and sink cells, $N_{a,\max}$ and $Q_{a,\max}$ are set as a large number, for the cells indicating the outer ring roads. For ordinary cells, $N_{a,\max}$ are determined by the maximum traffic flow rate of the road, and $Q_{a,\max}$ are determined by the length of the cell and the number of lanes, supposing 50 vehicles per km per lane at jam density. Therefore, for the cells representing outer ring roads, $N_{a,\max}= 1200, Q_{a,\max}= 720$, and for the inner road cells, $N_{a,\max}= 600, Q_{a,\max}= 360$.

Different numbers are assigned to different types of vehicles as indices and the weighting factors of them are listed in Table 6.

TABLE 6. Indices and weighting factors of different types of vehicles.

Type	c(Index)	w_c
MEG	1	10
MESS	2	10
RC	3	10
EB	4	8
Ordinary vehicle	5	1

Assume that when the extreme event happens, there are ordinary vehicles distributing at each road, and the initial $X^0_{a,5}$ for all ordinary cells are generated randomly in the interval $[0, Q_{a,\max}]$, as shown in Table 7. The initial $Y^0_{(a,b),c}$ are set as 0 for all connectors and all types of vehicles. It is assumed that there is a traffic jam in road 1-2 because of an accident.

For emergency vehicles, only the corresponding source cells have positive values of vehicles as listed in Table 8, while the values of other cells are all 0.

Apply the proposed WDTA model to obtain the optimal dynamic traffic assignment strategy, the results are illustrated in Table 9. It should be noted that the departure time is set for all dispatched vehicles because making decisions, sending orders, and preparing for departure cost time.

TABLE 7. Initial numbers of ordinary vehicles in each cell.

Cell (#)	$X_{a,5}^0$	Cell (#)	$X_{a,5}^0$	Cell (#)	$X_{a,5}^0$	Cell (#)	$X_{a,5}^0$
1	0	12	197	23	0	34	273
2	1034	13	345	24	285	35	268
3	1018	14	347	25	345	36	141
4	293	15	57	26	236	37	236
5	326	16	349	27	13	38	0
6	46	17	345	28	306	39	0
7	329	18	175	29	0	40	0
8	228	19	288	30	0	41	0
9	35	20	51	31	336		
10	100	21	152	32	244		
11	0	22	330	33	0		

TABLE 8. Initial numbers of emergency vehicles in source cells.

Cell 1			Cell 7	Cell 17	Cell 27
$X_{1,1}^0$	$X_{1,2}^0$	$X_{1,3}^0$	$X_{7,4}^0$	$X_{17,4}^0$	$X_{27,4}^0$
8	4	4	7	8	10

2) Step 2: Determine the Critical Load Restoration Strategy

Based on the results of Step 1, the multi-period restoration strategy is obtained for the distribution system. Whole outage duration is divided into 48 periods. Each period is as long as a time interval set in WDTA, i.e. 5min. The post-restoration state of the DS is shown in Fig. 7. Line 1-2 is determined to open and tie lines are closed. After solving the MILP, the objective value is 25668 and the computation time is 21.90s. The three-phase voltage profile in each period is in Fig.8. As it presents, the voltage magnitudes are within limits (0.95-1.05 p.u.) for all buses at all phases.

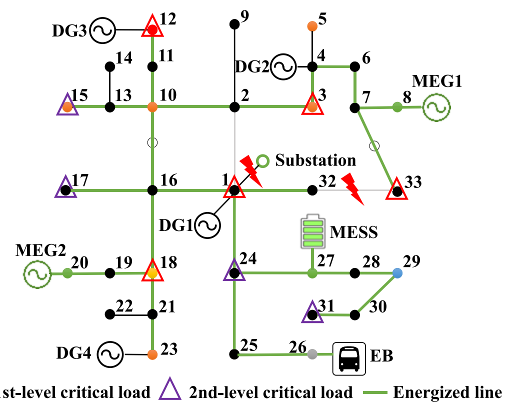

FIGURE 7. The post-restoration state of the DS.

The output and energy consumption results of each source are illustrated in Fig. 9, and the load restoration results are shown in Fig. 10.

From Fig. 9(a), at the beginning of the restoration, around 1-6 periods, the main sources to support restoration are local DGs. After the mobile sources arrive, they gradually become the main sources for service restoration. After 12 periods, all the local sources cannot support restoration any longer, and only the mobile sources support restoration. From Fig. 9(b), the energy in local DGs is nearly used up in period 12. MEGs nearly use up their energy in 48 periods (1200kWh for each bus). Both EBs and MESSs remain energy and energy consumption rates are both nearly 87.50%.

In Fig. 10, the sum of weighted restored load and the amount of restored load demand in each period are depicted by bar and line graphs respectively. In periods 1 and 2, the bar

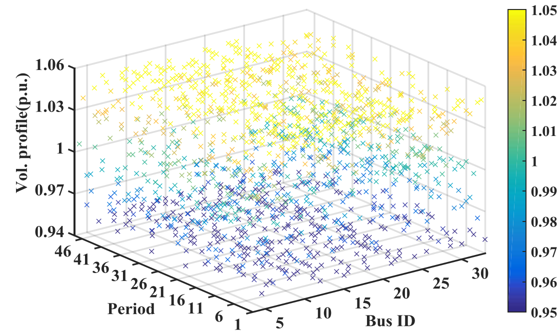

FIGURE 8. The three-phase voltage profile in each period.

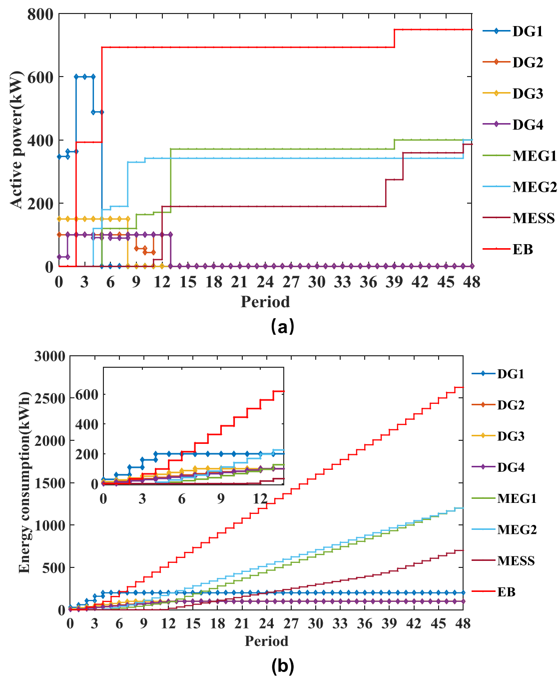

FIGURE 9. The output and energy consumption results for all sources. (a)The output results. (b) Energy consumption results.

TABLE 9. The routing and arrival time of vehicles.

Type	O-D pair	Routing	Departure time (min)	Arrival time (min)
MEG	1-6	1-4-5-6	5	25
	1-7	1-3-7	5	20
MESS	1-9	1-4-8-9	5	30
RC	1-10	1-4-5-9-10	5	35
EB	13-12	13-5-9-12	5	20
	14-12	14-7-11-12	5	20
	15-12	15-12	5	10

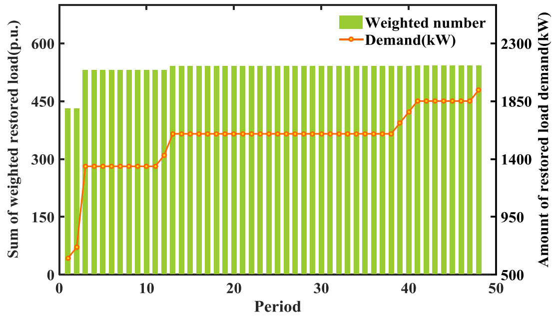

FIGURE 10. The load restoration results in each period.

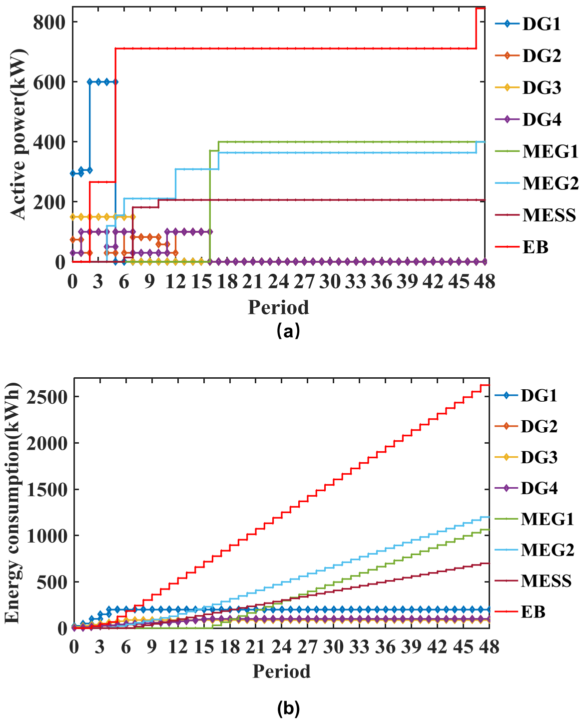

FIGURE 11. The output and energy consumption results for all sources in Case I. (a)The output results. (b) Energy consumption results.

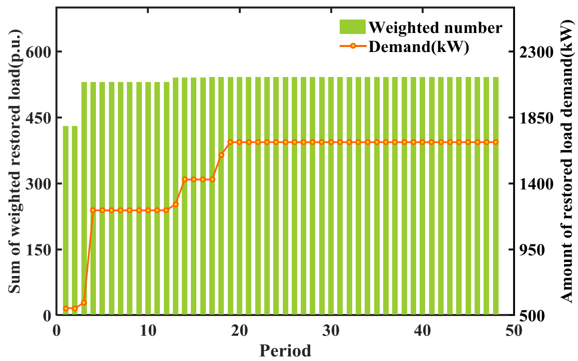

FIGURE 12. The load restoration results in each period in Case I.

changes little because a regular load is picked up in period 2, which will make little impact on the sum of weighted restored load (with weighting factor 0.2). In period 3, the 1st-level critical load at bus 1 is picked up. It is not restored in period 1 because it is large and at the beginning of the restoration, the mobile sources are absent and power energy is limited. In periods 12 and 13, the bar changes visibly because the faulted zone is energized, then the 2nd-level load 31 and regular load 30 are picked up.

C. COMPARISONS

Take the case in last part as the *Base Case*, and this part will compare it with two cases, i.e., *Case I* with routing the mobile sources by the shortest path used in many papers, and *Case II* without the support of EBs.

1) Case I: Routing by Shortest Path

In this case, the routing strategy is obtained by finding the shortest path in O-D of sources. By using this method, the route and arrival time of MEGs to destination 6 will be different from those in the *Base Case*.The route for MEGs to destination 6 is 1-2-6. According to Greenshields' model [34], for cell 2 and 3, the speed can be calculated by

$$V_a = V_{a,\max}\left(1 - N_a/N_{a,\max}\right), a \in \mathcal{C} \tag{7}$$

where $V_{a,\max}$ is the free speed of the corresponding road, and N_a is the vehicle number in cell a, indicating the density. Then the time from 1 to 2 is 69.11min. Therefore, the arrival time for MEGs to destination 6 is 79.11min. Based on the results in the TS, the multi-period restoration strategy for the DS can be obtained. The output and energy consumption results of each source are illustrated in Fig. 11, and the load restoration results are shown in Fig. 12.

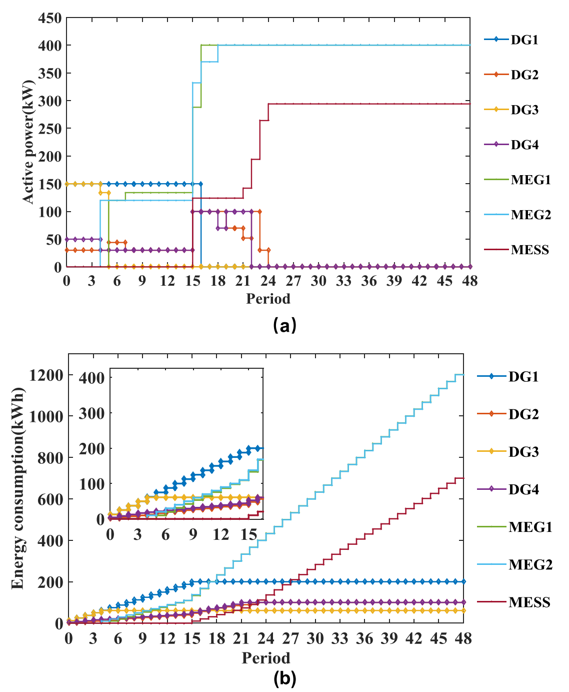

FIGURE 13. The output and energy consumption results for all sources in Case II. (a)The output results. (b) Energy consumption results.

The objective value is 25662.6 and similar to that in *Base Case*, as the total generation resource is relatively enough

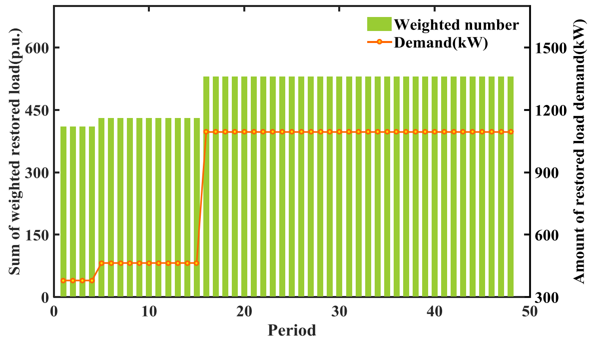

FIGURE 14. The load restoration results in each period in Case II.

TABLE 10. The information of spot loads.

Node (#)	Ph-1 (kW)	Ph-1 (kVar)	Ph-2 (kW)	Ph-2 (kVar)	Ph-3 (kW)	Ph-3 (kVar)
1	140	70	140	70	350	175
2	0	0	0	0	0	0
3	0	0	0	0	85	40
4	0	0	0	0	42	21
5	17	8	21	10	0	0
6	0	0	0	0	85	40
7	0	0	0	0	0	0
8	0	0	140	70	21	10
9	0	0	0	0	85	40
10	0	0	0	0	0	0
11	0	0	0	0	42	21
12	42	21	42	21	42	21
13	85	40	0	0	0	0
14	0	0	0	0	0	0
15	42	21	0	0	0	0
16	0	0	0	0	85	40
17	0	0	42	21	0	0
18	0	0	42	21	0	0
19	0	0	0	0	0	0
20	8	4	85	40	0	0
21	0	0	0	0	0	0
22	0	0	0	0	0	0
23	0	0	85	40	0	0
24	0	0	0	0	42	21
25	85	40	0	0	0	0
26	0	0	0	0	0	0
27	0	0	0	0	42	21
28	0	0	0	0	85	40
29	140	70	0	0	0	0
30	0	0	42	21	0	0
31	126	62	0	0	0	0
32	0	0	0	0	0	0
33	0	0	0	0	85	40

to supply power to all critical loads. However, the total restored energy is 6076.42kWh, while that in *Base Case* is 6244.33 kWh. It is because more regular loads are supplied in *Base Case*.

2) Case II: Without Support of EB

In this case, the EBs are not utilized for service restoration. The multi-period restoration strategy for the DS can be obtained. The output and energy consumption results of each source are illustrated in Fig. 13, and the load restoration results are shown in Fig. 14.

TABLE 11. The information of lines.

i (#)	j (#)	Length (ft.)	Config.	i (#)	j (#)	Length (ft.)	Config.
1	2	960	722	18	19	320	723
2	3	400	724	18	21	200	724
3	4	360	723	19	20	1280	724
4	5	1320	722	21	22	400	723
4	6	240	724	21	23	200	724
6	7	600	723	1	24	520	723
7	8	80	724	24	25	520	724
2	9	800	723	24	27	920	724
2	10	320	722	25	26	600	723
10	11	240	724	27	28	280	723
11	12	280	724	28	29	200	723
10	13	760	724	29	30	640	723
13	14	120	724	30	31	200	724
13	15	320	723	1	32	520	724
1	16	200	722	7	33	100	1
16	17	320	724	10	16	100	1
16	18	600	723				

The objective value is 23860 and 92.96% of that in *Base Case*. In addition, the total restored energy is 3560.50kWh, 42.98% less than that in *Base Case*. It is because, without the support of EBs, less critical loads are restored. To sum up, the support of EBs is essential for the restoration

VII. CONCLUSION AND FUTURE WORK

This paper proposes a resilience-oriented service restoration framework for distribution systems considering the dispatch of mobile emergency resources in the transportation system. The two-step framework includes a weighted dynamic traffic assignment model in step 1 to determine the routes and travel time of mobile emergency sources, and a critical load restoration model to determine the multi-period restoration strategy in step 2. The case studies indicate that the proposed method is effective and efficient. In addition, it illustrates that considering the traffic state is important because congestion in the TS may delay the restoration process. EBs are essential for service restoration due to their relatively large capacities and flexibility.

In the future, the interdependency between electric power systems and other critical infrastructures, such as the natural gas system [36] and the communication system, will be considered when making decisions on critical load restoration strategy. In addition, the social function of critical loads, such as hospitals, should be taken into account in the objective functions to make the reservice restoration strategy more practical.

APPENDIX

The basic data for the distribution system in this paper are from the IEEE 37 node test feeder, the specific information is given in Table 10 and 11.

In Table 10, all loads are modeled as PQ load. In Table 11, the entry "Config." indicates the configuration ID of the lines, which can be found in [35]. For tie lines, the "config.1" means the lines with $(0.2 + 0.8j)$ in ohms per mile.

REFERENCES

[1] Y. Wang, C. Chen, J. Wang, and R. Baldick, "Research on resilience of power systems under natural disasters—A review," *IEEE Trans. Power Syst.*, vol. 31, no. 2, pp. 1604–1613, Mar. 2016.
[2] Office of the Press Secretary of the White House. *Presidential Policy Directive—Critical Infrastructure Security and Resilience*. Accessed: Jul. 2017. [Online]. Available: http://www.whitehouse.gov/the-press-office/2013/02/12/presidential-policy-directive-critical-infrastructure-security-and-resil
[3] B. Cai, M. Xie, Y. Liu, Y. Liu, and Q. Feng, "Availability-based engineering resilience metric and its corresponding evaluation methodology," *Rel. Eng. Syst. Saf.*, vol. 172, pp. 216–224, Apr. 2018.
[4] Q. Feng, X. Zhao, D. Fan, B. Cai, Y. Liu, and Y. Ren, "Resilience design method based on meta-structure: A case study of offshore wind farm," *Rel. Eng. Syst. Saf.*, vol. 186, pp. 232–244, Jun. 2019.
[5] D. Ton and W.-T. P. Wang, "A more resilient grid: The U.S. department of energy joins with stakeholders in an R&D plan," *IEEE Power Energy Mag.*, vol. 13, no. 3, pp. 26–34, May/Jun. 2015.
[6] Y. Ren, D. Fan, Q. Feng, Z. Wang, B. Sun, and D. Yang, "Agent-based restoration approach for reliability with load balancing on smart grids," *Appl. Energy*, vol. 249, pp. 46–57, Sep. 2019.
[7] Y. Xu, C.-C. Liu, Z. Wang, K. Mo, K. P. Schneider, F. K. Tuffner, and D. T. Ton, "DGs for service restoration to critical loads in a secondary network," *IEEE Trans. Smart Grid*, vol. 10, no. 1, pp. 435–447, Jan. 2019.
[8] Y. Xu, C.-C. Liu, K. P. Schneider, F. K. Tuffner, and D. T. Ton, "Microgrids for service restoration to critical load in a resilient distribution system," *IEEE Trans. Smart Grid*, vol. 9, no. 1, pp. 426–437, Jan. 2018.
[9] J. Li, X.-Y. Ma, C.-C. Liu, and K. P. Schneider, "Distribution system restoration with microgrids using spanning tree search," *IEEE Trans. Power Syst.*, vol. 29, no. 6, pp. 3021–3029, Nov. 2014.
[10] Z. Wang, C. Shen, Y. Xu, F. Liu, X. Wu, and C.-C. Liu, "Risk-limiting load restoration for resilience enhancement with intermittent energy resources," *IEEE Trans. Smart Grid*, vol. 10, no. 3, pp. 2507–2522, May 2019.
[11] Y. Wang, Y. Xu, J. He, C. C. Liu, K. P. Schneider, M. Hong, and D. T. Ton, "Coordinating multiple sources for service restoration to enhance resilience of distribution systems," *IEEE Trans. Smart Grid*, to be published. doi: 10.1109/TSG.2019.2891515.
[12] C. Chen, J. Wang, F. Qiu, and D. Zhao, "Resilient distribution system by microgrids formation after natural disasters," *IEEE Trans. Smart Grid*, vol. 7, no. 2, pp. 958–966, Mar. 2016.
[13] B. Chen, C. Chen, J. Wang, and K. L. Butler-Purry, "Sequential service restoration for unbalanced distribution systems and microgrids," *IEEE Trans. Power Syst.*, vol. 33, no. 2, pp. 1507–1520, Mar. 2018.
[14] A. Arif and Z. Wang, "Networked microgrids for service restoration in resilient distribution systems," *IET Gener., Transmiss. Distrib.*, vol. 11, no. 14, pp. 3612–3619, Sep. 2017.
[15] Z. Wang, B. Chen, J. Wang, and C. Chen, "Networked microgrids for self-healing power systems," *IEEE Trans. Smart Grid*, vol. 7, no. 1, pp. 310–319, Jan. 2016.
[16] N. T. Raknes, K. Ødeskaug, M. Stålhane, and L. Hvattum, "Scheduling of maintenance tasks and routing of a joint vessel fleet for multiple offshore wind farms," *J. Mar. Sci. Eng.*, vol. 5, no. 1, pp. 1–25, Feb. 2017.
[17] S. Lei, C. Chen, H. Zhou, and Y. Hou, "Routing and scheduling of mobile power sources for distribution system resilience enhancement," *IEEE Trans. Smart Grid*, to be published. doi: 10.1109/TSG.2018.2889347.
[18] H. Gao, Y. Chen, S. Mei, S. Huang, and Y. Xu, "Resilience-oriented pre-hurricane resource allocation in distribution systems considering electric buses," *Proc. IEEE*, vol. 105, no. 7, pp. 1214–1233, Jul. 2017.
[19] S. Lei, J. Wang, C. Chen, and Y. Hou, "Mobile emergency generator pre-positioning and real-time allocation for resilient response to natural disasters," *IEEE Trans. Smart Grid*, vol. 9, no. 3, pp. 2030–2041, May 2018.
[20] J. Kim and Y. Dvorkin, "Enhancing distribution system resilience with mobile energy storage and microgrids," *IEEE Trans. Smart Grid*, to be published. doi: 10.1109/TSG.2018.2872521.
[21] A. Arif, Z. Wang, J. Wang, and C. Chen, "Power distribution system outage management with co-optimization of repairs, reconfiguration, and DG dispatch," *IEEE Trans. Smart Grid*, vol. 9, no. 5, pp. 4109–4118, Sep. 2018.
[22] A. Kavousi-Fard, M. Wang, and W. Su, "Stochastic resilient post-hurricane power system recovery based on mobile emergency resources and reconfigurable networked microgrids," *IEEE Access*, vol. 6, pp. 72311–72326, 2018.
[23] S. Yao, P. Wang, and T. Zhao, "Transportable energy storage for more resilient distribution systems with multiple microgrids," *IEEE Trans. Smart Grid*, vol. 10, no. 3, pp. 3331–3341, May 2019.
[24] W. Wei, S. Mei, L. Wu, J. Wang, and Y. Fang, "Robust operation of distribution networks coupled with urban transportation infrastructures," *IEEE Trans. Power Syst.*, vol. 21, no. 3, pp. 2118–2130, May 2017.
[25] Z. Shao, Z. Ma, S. Liu, and T. Lv, "Optimization of a traffic control scheme for a post-disaster urban road network," *Sustainability*, vol. 10, no. 1, pp. 1–22, Jan. 2018.
[26] W. Wei and D. Wu, "Interdependence between transportation system and power distribution system: A comprehensive review on models and applications," *Power Syst. Clean Energy*, vol. 7, no. 3, pp. 433–448, May 2019.
[27] C. F. Daganzo, "The cell transmission model, part II: Network traffic," *Transp. Res. B, Methodol.*, vol. 39, no. 1, pp. 79–93, Apr. 1995.
[28] X. Wang, M. Shahidehpour, C. Jiang, and Z. Li, "Resilience enhancement strategies for power distribution network coupled with urban transportation system," *IEEE Trans. Smart Grid*, to be published. doi: 10.1109/TSG.2018.2848970.
[29] A. K. Ziliaskopoulos, "A linear programming model for the single destination system optimum dynamic traffic assignment problem," *Transp. Sci.*, vol. 34, no. 1, pp. 37–49, 2000.
[30] Y.-C. Chiu and H. Zheng, "Real-time mobilization decisions for multi-priority emergency response resources and evacuation groups: Model formulation and solution," *Transp. Res. E, Logistics Transp. Rev.*, vol. 43, no. 6, pp. 710–736, Nov. 2007.
[31] *CVX: MATLAB Software for Disciplined Convex Programming*. Accessed: Mar. 2017. [Online]. Available: http://cvxr.com/cvx/
[32] *MOSEK Fusion API for MATLAB 8.1.0.41*. Accessed: Mar. 2017. [Online]. Available: http://docs.mosek.com/8.1/matlabfusion/index.html
[33] L. Gan and S. H. Low, "Convex relaxations and linear approximation for optimal power flow in multiphase radial networks," in *Proc. Power Syst. Comput. Conf. (PSCC)*, Wrocław, Poland, Aug. 2014, pp. 1–9.
[34] B. D. Greenshields, J. R. Bibbins, W. S. Channing, and H. H. Miller, "A study of traffic capacity," in *Proc. Highway Res. Board*, vol. 14, 1935, pp. 448–477.
[35] K. P. Schneider, B. A. Mather, B. C. Pal, C. W. Ten, G. J. Shirek, H. Zhu, J. C. Fuller, J. L. R. Pereira, L. F. Ochoa, L. R. de Araujo, R. C. Dugan, S. Matthias, S. Paudyal, T. E. McDermott, and W. Kersting, "Analytic considerations and design basis for the IEEE distribution test feeders," *IEEE Trans. Power Syst.*, vol. 33, no. 3, pp. 3181–3188, May 2018.
[36] T. O. Trifonov, "Coordination of battery energy storage and power-to-gas in distribution systems," *Protection Control Mod. Power Syst.*, vol. 2, no. 1, pp. 1–38, 2017.

YIN XU (S'12–M'14–SM'18) received the B.E. and Ph.D. degrees in electrical engineering from Tsinghua University, Beijing, China, in 2008 and 2013, respectively.

From 2013 to 2016, he was an Assistant Research Professor with the School of Electrical Engineering and Computer Science, Washington State University, Pullman, WA, USA. He is currently a Professor with Beijing Jiaotong University, Beijing. His research interests include power system resilience, distribution system restoration, and power systems electromagnetic transient simulation.

Dr. Xu is currently serving as Secretary of the Distribution Test Feeder Working Group under the IEEE PES Distribution System Analysis Subcommittee.

YING WANG (S'16) received the B.E. degree in electrical engineering from Beijing Jiaotong University, Beijing, China, in 2014, where she is currently pursuing the Ph.D. degree. From 2017 to 2018, she was a Visiting Scholar with Case Western Reserve University, Cleveland, OH, USA. Her research interests include distribution system restoration and power system resilience.

JINGHAN HE (M'07–SM'18) received the M.Sc. degree in automation from Tianjin University, Tianjin, China, in 1994, and the Ph.D. degree in electrical engineering from Beijing Jiaotong University, Beijing, China, in 2007. She is currently a Professor with Beijing Jiaotong University. Her main research interests include protective relaying, fault distance measurement, and location in power systems.

MINGYU SU received the B.E. degree in electrical engineering from Beijing Jiaotong University, Beijing, China, in 2017, where she is currently pursuing the M.Sc. degree. Her research interests include distribution system restoration and power system resilience.

PINGHAO NI received the M.Sc. degree in power system and automation from the China Electric Power Research Institute, Beijing, China. He is currently a Senior Experimentalist with the School of Electrical Engineering, Beijing Jiaotong University, Beijing. His research interest includes power system and automation.